Stochastic framework for modeling the linear apparent behavior of complex materials: application to random porous materials with interphases

J. Guilleminot*, T. T. Le , C. Soize

Université Paris-Est
Laboratoire Modélisation et Simulation Multi Echelle, MSME UMR8208 CNRS
5 Bd Descartes, 77454 Marne la Vallée
France

This work[1] was supported by the French National Research Agency (ANR) under grant ANR-12-JS09-0001-01.

Abstract

This paper is concerned with the modeling of randomness in multiscale analysis of heterogeneous materials. More specifically, a framework dedicated to the stochastic modeling of random properties is first introduced. A probabilistic model for matrix-valued second-order random fields with symmetry propertries, recently proposed in the literature, is further reviewed. Algorithms adapted to the Monte Carlo simulation of the proposed representation are also provided. The derivations and calibration procedure are finally exemplified through the modeling of the apparent properties associated with an elastic porous microstructure containing stochastic interphases.

Keywords

Apparent properties; MaxEnt; Probabilistic model.

1 Introduction

In this paper, we address the modeling of randomness in multiscale analysis of heterogeneous materials. Such an issue naturally arises when one is concerned with random materials, in which case the randomness

*Corresponding author: johann.guilleminot@univ-paris-est.fr

[1]**Preprint version**. Accepted for publication in Acta Mechanica Sinica on November 12th 2013.

is usually related to the description of the underlying microstructure [12]. In the framework of mean-field homogenization theories, such information is typically taken into account, for particulate microstructures, through a description of the characteristic functions associated with the different types of inclusions (see [21] for an extensive review). In effect, the complexity of such a description makes it be restricted to microstructures satisfying a few simplifying assumptions, such as statistical homogeneity and isotropy. From a computational standpoint, the random morphology can be accounted for by having recourse to advanced representation techniques, among which the use of random set models (in connection with concepts derived from mathematical morphology [14]) or parametric probabilistic models in high dimensions (see e.g. [1], as well as [22] for the modeling of random phase properties at microscale for instance). Indeed, the choice of a suitable representation is often guided by the amount and nature of data available.

In this context, and while the development of sophisticated experimental techniques (such as tomography) has made the description of materials at an unprecedented level of resolution possible, the number and size of samples are still rather limited, hence making the identification of the above models difficult. Alternatively, one may choose to represent the random medium through some of its properties (e.g. an elasticity or a permeability tensor) defined at a coarser, mesoscopic scale. These properties then exhibit smoother statistical fluctuations (in comparison to the ones occurring at the finest scale observable) and can be used as input data for computational upscaling. In addition, they generally depend on parameters living in low-dimensional spaces and can therefore be identified solving statistical inverse problems. Such representations were recently applied for the analysis of the representative volument element size associated with an anisotropic elastic microstructure [19] and for elastic wave propagation in random media [20], for instance.

The goal of this work is twofold. First, it aims at presenting in a very simple form a general methodology that allows for the construction of probabilistic models for the aforementionned random properties. This approach, while used quite extensively (in its random matrix form) by the community of uncertainty quantification for the analysis of random dynamical systems exhibiting both model and parametric uncertainties [16], has received somewhat little attention by researchers involved in multiscale analysis of random media. It is our purpose here to demonstrate some of the main capabilities of this framework. Second, we investigate the behavior and identification of the proposed model for the modeling of a random porous material containing stochastic heterogeneous interphases. At this stage, it is worth pointing out that the proposed methodology, while formulated hereinafter for the modeling of elasticity matrix random fields, can be readily applied (up to some technical adaptations) to the modeling of any physical quantity associated with a random material. More precisely, we address the modeling of elasticity tensor random fields, for which:

- The stochastic elasticity tensor is close to a given material symmetry in mean, but exhibits more or less anisotropic fluctuations around this symmetry class.
- The level of statistical fluctuations of the random tensor and that of a stochastic anitropy measure must be controled apart from each other.

Such specifications are of interest in a wide range of situations, among which the modeling of apparent elastic properties (defined at some mesoscale) or the modeling of epistemic uncertainties (regardless of whether the scales are separated or not) that may arise whenever experimental results are involved. The methodology

and algorithms are therefore intended as useful for both theoreticians and experimentalists involved in the analysis, modeling and testing of complex materials.

The rest of the paper is organized as follows. The overall methodology is first presented in section 2, where the generalized stochastic model derived in [7] is recalled in a form stripped of mathematical details. The associated random generation algorithms are then presented in section 3. The use of the model for the computational multiscale analysis of an elastic microstructure is finally exemplified in section 4.

2 Prior stochastic model for matrix-valued non-Gaussian random fields

We introduce for later reference the following matrix sets:

- $\mathbb{M}_n(\mathbb{R})$: the set of all the n-by-n real matrices.
- $\mathbb{M}_n^S(\mathbb{R})$: the set of all the symmetric n-by-n real matrices.
- $\mathbb{M}_n^+(\mathbb{R})$: the set of all the positive-definite symmetric n-by-n real matrices.
- $\mathbb{M}_n^{\rm sym}(\mathbb{R})$: the set of all the positive-definite symmetric n-by-n real matrices representing elasticity matrices (defined with respect to the Kelvin-Voigt notation) exhibiting the material symmetry "sym".

One has $\mathbb{M}_n^{\rm sym}(\mathbb{R}) \subset \mathbb{M}_n^+(\mathbb{R}) \subset \mathbb{M}_n^S(\mathbb{R}) \subset \mathbb{M}_n(\mathbb{R})$. Throughout the paper, the notation "c" denotes normalization constants whose values may change from line to line. Finally, $\mathbb{E}$ is the mathematical expectation.

2.1 Overview of the construction

Let Ω be an open bounded domain in $\mathbb{R}^d$, $1 \leqslant d \leqslant 3$. In what follows, we denote by $\{[\boldsymbol{C}(\boldsymbol{x})], \boldsymbol{x} \in \Omega\}$ the $\mathbb{M}_n^+(\mathbb{R})$-valued second-order random field (defined on some probability space $(\Theta, \mathcal{T}, P)$) whose probabilistic model has to be constructed. To this aim, we follow the following two-step strategy (see [17], as well as [3–4–7] for various extensions).

In a first step, the family $\{p_{[\boldsymbol{C}(\boldsymbol{x})]}\}_{\boldsymbol{x}}$ of first-order marginal probability distributions associated with the aforementionned random field is constructed by using the maximum entropy (MaxEnt) principle, introduced by Jaynes in the 1950s [2–3]. In order to achieve such a construction, it is assumed that some objective information on random variable $[\boldsymbol{C}(\boldsymbol{x})]$ is available and can be expressed, for any $\boldsymbol{x}$ fixed in Ω, through a set of μ constraint equations (in addition to the usual normalization constraint)

$$\begin{aligned} \mathbb{E}\{\phi_1([\boldsymbol{C}(\boldsymbol{x})])\} &= h_1(\boldsymbol{x}) \,, \\ &\dots \\ \mathbb{E}\{\phi_\mu([\boldsymbol{C}(\boldsymbol{x})])\} &= h_\mu(\boldsymbol{x}) \,, \end{aligned} \tag{1}$$

in which $\mathbb{E}$ is the mathematical expectation, $\phi_1, \dots, \phi_\mu$ are μ measurable functions defined from $\mathbb{M}_n^+(\mathbb{R})$ into some subsets $\mathbb{H}_1, \dots, \mathbb{H}_\mu$ of $\mathbb{M}_n(\mathbb{R})$ and $h_1(\boldsymbol{x}), \dots, h_\mu(\boldsymbol{x})$ are given deterministic quantities in $\mathbb{H}_1, \dots, \mathbb{H}_\mu$. For

instance, setting any of the above functions as the identity function allows one to prescribe the mean value of $[\boldsymbol{C}(\boldsymbol{x})]$ at point $\boldsymbol{x}$. The maximum entropy principle states that among all the probability density functions satisfying the above constraints, the one which should be selected is the one that maximizes the uncertainties (as measured by Shannon's entropy [15]), hence providing a model that is expected to be as objective as possible. Solving this optimization problem by the method of Lagrange multipliers, it can easily be shown that the MaxEnt-based probability density function (p.d.f.) $p_{[\boldsymbol{C}(\boldsymbol{x})]}$ of random variable $[\boldsymbol{C}(\boldsymbol{x})]$ is defined as

$$p_{[\boldsymbol{C}(\boldsymbol{x})]}([C]) = \mathcal{I}_{\mathbb{M}_n^+(\mathbb{R})}([C])\; c\; \exp\left\{ - \sum_{i=1}^{\mu} < \Lambda_i, \phi_i([C]) > \right\} , \tag{2}$$

in which $\mathcal{I}_{\mathbb{M}_n^+(\mathbb{R})}$ is the indicator function of matrix set $\mathbb{M}_n^+(\mathbb{R})$, Λ_i is the Lagrange multiplier associated with the i-th constraint and $< \cdot, \cdot >$ is the inner product in $\mathbb{M}_n(\mathbb{R})$. One should note that the Lagrange multipliers belong to some admissible sets, the definition of which must ensure the integrability of $p_{[\boldsymbol{C}(\boldsymbol{x})]}$. The construction of the family $\{p_{[\boldsymbol{C}(\boldsymbol{x})]}\}_{\boldsymbol{x}}$ is specifically addressed in sections 2.2 and 2.3.

In a second step, the random field $\{[\boldsymbol{C}(\boldsymbol{x})], \boldsymbol{x} \in \Omega\}$ is expressed through a nonlinear mapping acting on a set of independent second-order centered homogeneous real-valued Gaussian random fields and such that $\{[\boldsymbol{C}(\boldsymbol{x})], \boldsymbol{x} \in \Omega\}$ exhibits the target system of first-order marginal probability distributions. It is worth pointing out that $\{[\boldsymbol{C}(\boldsymbol{x})], \boldsymbol{x} \in \Omega\}$ then inherits some correlation structure which is induced by the transformation of the correlation structures of the underlying Gaussian random fields. In practice, the nonlinear mapping can be either defined in a closed-form and as a memoryless transformation for a few particular cases, or defined as a transformation with memory for more general cases (see section 3.2).

2.2 Prior algebraic representation

For all $\boldsymbol{x}$ fixed in Ω, the second-order random matrix $[\boldsymbol{C}(\boldsymbol{x})]$ is first decomposed as [7]

$$[\boldsymbol{C}(\boldsymbol{x})] = [\boldsymbol{M}(\boldsymbol{x})]^{1/2}\, [\boldsymbol{A}(\boldsymbol{x})]\, [\boldsymbol{M}(\boldsymbol{x})]^{1/2} , \tag{3}$$

where:

- $\{[\boldsymbol{A}(\boldsymbol{x})], \boldsymbol{x} \in \Omega\}$ is a $\mathbb{M}_n^+(\mathbb{R})$-valued second-order normalized random field (with purely anisotropic fluctuations) belonging to the class SFE^+ of random fields defined in [17].
- $\{[\boldsymbol{M}(\boldsymbol{x})], \boldsymbol{x} \in \Omega\}$ is a $\mathbb{M}_n^{\mathrm{sym}}(\mathbb{R})$-valued second-order random field, statistically independent of $\{[\boldsymbol{A}(\boldsymbol{x})], \boldsymbol{x} \in \Omega\}$ and exhibiting $\mathbb{M}_n^{\mathrm{sym}}(\mathbb{R})$-valued fluctuations.

More specifically, and for construction purposes, the random matrix $[\boldsymbol{M}(\boldsymbol{x})]$ is defined as

$$[\boldsymbol{M}(\boldsymbol{x})] = [\underline{C}^{\mathrm{sym}}(\boldsymbol{x})]^{1/2}\; \exp\{[\boldsymbol{G}(\boldsymbol{x})]\}\, [\underline{C}^{\mathrm{sym}}(\boldsymbol{x})]^{1/2} , \tag{4}$$

in which

- $[\underline{C}^{\mathrm{sym}}(\boldsymbol{x})] = [P^{\mathrm{sym}}([\underline{C}(\boldsymbol{x})])]$, with $[\underline{C}(\boldsymbol{x})] = \mathbb{E}\{[\boldsymbol{C}(\boldsymbol{x})]\}$ and P^{sym} the projection operator from $\mathbb{M}_n^+(\mathbb{R})$ onto $\mathbb{M}_n^{\mathrm{sym}}(\mathbb{R})$.
- $\{[\boldsymbol{G}(\boldsymbol{x})], \boldsymbol{x} \in \Omega\}$ is an auxiliary $\mathbb{M}_n^S(\mathbb{R})$-valued random field that is statistically independent of random field $\{[\boldsymbol{A}(\boldsymbol{x})], \boldsymbol{x} \in \Omega\}$.

As for the scalar case, the matrix exponential is used in order to relax the positive-definiteness constraint. The phenomenological decomposition given by Eq. (3) allows for some uncoupling between the level of statistical fluctuations of $[\boldsymbol{C}(\boldsymbol{x})]$ and its level of stochastic anisotropy, and yields some flexibility in the modeling of anisotropy through up- and downscaling [7].

2.3 Definition of the families of first-order marginal probability distributions

From Eqs. (3) and (4), it is clear that the p.d.f. $p_{[\boldsymbol{C}(\boldsymbol{x})]}$ of $[\boldsymbol{C}(\boldsymbol{x})]$ depends on the two p.d.f. associated with random variables $[\boldsymbol{M}(\boldsymbol{x})]$ and $[\boldsymbol{A}(\boldsymbol{x})]$. These two p.d.f. are constructed in the next two sections, making use of the MaxEnt principle briefly introduced in section 2.1.

2.3.1 Probability distribution of random matrix $[\boldsymbol{A}(\boldsymbol{x})]$

For $\boldsymbol{x}$ fixed in Ω, let $p_{[\boldsymbol{A}(\boldsymbol{x})]}$ be the probability density function of the $\mathbb{M}_n^+(\mathbb{R})$-valued random variable $[\boldsymbol{A}(\boldsymbol{x})]$. Following section 2.1, this p.d.f. can be constructed by having recourse to the MaxEnt principle, for which some algebraic constraints synthesizing the available information must be defined. In this work, the normalization condition for $p_{[\boldsymbol{A}(\boldsymbol{x})]}$, together with the following constraints

(i) $\mathbb{E}\{[\boldsymbol{A}(\boldsymbol{x})]\} = [\underline{C}^{\mathrm{sym}}(\boldsymbol{x})]^{-1/2}\,[\underline{C}(\boldsymbol{x})]\,[\underline{C}^{\mathrm{sym}}(\boldsymbol{x})]^{-1/2}$,

(ii) $\mathbb{E}\{\log(\det([\boldsymbol{A}(\boldsymbol{x})]))\} = \nu_{[\boldsymbol{A}]}(\boldsymbol{x})$, $|\nu_{[\boldsymbol{A}]}(\boldsymbol{x})| < +\infty$,

are considered, for all $\boldsymbol{x}$ in Ω. For later use, we let $\mathbb{E}\{[\boldsymbol{A}(\boldsymbol{x})]\} = [\underline{A}(\boldsymbol{x})]$ and introduce the following Cholesky decomposition of mean matrix $[\underline{A}(\boldsymbol{x})]$: $[\underline{A}(\boldsymbol{x})] = [\underline{L}(\boldsymbol{x})]^{\mathrm{T}}\,[\underline{L}(\boldsymbol{x})]$. The first constraint readily follows from Eqs. (3) and (4), while the second one implies that $[\boldsymbol{A}(\boldsymbol{x})]$ and its inverse are both second-order random variables [17]. Note that when $[\underline{C}(\boldsymbol{x})] \in \mathbb{M}_n^{\mathrm{sym}}(\mathbb{R})$, the first equation simply reduces to $\mathbb{E}\{[\boldsymbol{A}(\boldsymbol{x})]\} = [I_n]$. It can then be shown that the MaxEnt-based p.d.f. $p_{[\boldsymbol{A}(\boldsymbol{x})]}$ of $[\boldsymbol{A}(\boldsymbol{x})]$ reads as

$$p_{[\boldsymbol{A}(\boldsymbol{x})]}([A]) = \mathcal{I}_{\mathbb{M}_n^+(\mathbb{R})}([A])\; c\;\det([A])^{\ell_1(\boldsymbol{x})}\;\exp\left\{-\ell_2(\boldsymbol{x})\,\mathrm{tr}([\underline{A}(\boldsymbol{x})]^{-1}[A])\right\} \tag{5}$$

in which

$$\ell_1(\boldsymbol{x}) = (n+1)(1-\delta(\boldsymbol{x})^2)/(2\delta(\boldsymbol{x})^2)\;,\quad \ell_2(\boldsymbol{x}) = (n-1)/(2\delta(\boldsymbol{x})^2)\;, \tag{6}$$

and $\delta(\boldsymbol{x})$ is a model parameter measuring the dispersion of random variable $[\boldsymbol{A}(\boldsymbol{x})]$:

$$\delta(\boldsymbol{x}) = \left\{\mathbb{E}\{\|[\boldsymbol{A}(\boldsymbol{x})] - [\underline{A}(\boldsymbol{x})]\|_{\mathrm{F}}^2\}/n\right\}^{1/2}\;. \tag{7}$$

2.3.2 Probability distribution of random matrix $[\boldsymbol{G}(\boldsymbol{x})]$

Let $\{E_i\}_{i=1}^N$ be the basis of matrix set $\mathbb{M}_n^{\mathrm{sym}}(\mathbb{R})$, defined as the matrix representation of Walpole's tensor basis associated with the material symmetry "sym" [24]. The $\mathbb{M}_n^S(\mathbb{R})$-valued random variable $[\boldsymbol{G}(\boldsymbol{x})]$ is thus written as

$$\forall \boldsymbol{x} \in \Omega, \quad [\boldsymbol{G}(\boldsymbol{x})] = \sum_{i=1}^{N} G_i(\boldsymbol{x})\, [E_i]\,, \tag{8}$$

where $\forall i \in \{1, \ldots, N\}$, $G_i(\boldsymbol{x}) \in \mathbb{R}$. Making use of the results derived in [24], it can be shown that $\exp\{[\boldsymbol{G}(\boldsymbol{x})]\}$ is a $\mathbb{M}_n^{\mathrm{sym}}(\mathbb{R})$-valued random variable. We then consider the construction of a stochastic model for the $\mathbb{R}^N$-valued random variable $\boldsymbol{G}(\boldsymbol{x}) = (G_1(\boldsymbol{x}), \ldots, G_N(\boldsymbol{x}))$, the probability density function of which is denoted by $p_{\boldsymbol{G}(\boldsymbol{x})}$. It is assumed that $\boldsymbol{G}(\boldsymbol{x})$ is such that $\exp\{[\boldsymbol{G}(\boldsymbol{x})]\}$ satisfies a set of constraints that are similar to those satisfied by the anisotropic germ $[\boldsymbol{A}(\boldsymbol{x})]$, namely that

$$\mathbb{E}\left\{\exp\left(\sum_{i=1}^{N} G_i(\boldsymbol{x})[E_i]\right)\right\} = [I_n] \tag{9}$$

and

$$\sum_{i=1}^{N} \mathbb{E}\left\{G_i(\boldsymbol{x})\right\} \mathrm{tr}([E_i]) = \nu(\boldsymbol{x}),\ |\nu(\boldsymbol{x})| < +\infty\,. \tag{10}$$

Substituting Eq. (9) into Eq. (4) and taking mathematical expectation on both sides yields

$$\mathbb{E}\{[\boldsymbol{M}(\boldsymbol{x})]\} = [\underline{C}^{\mathrm{sym}}(\boldsymbol{x})]\,, \tag{11}$$

while the property given by Eq. (10) implies that $\exp\{[\boldsymbol{G}(\boldsymbol{x})]\}$ and its inverse are second-order random variables. Furthermore, it can be shown that $[\boldsymbol{G}(\boldsymbol{x})]$ is then a second-order random variable. It follows that the MaxEnt-based marginal p.d.f. $\boldsymbol{g} \mapsto p_{\boldsymbol{G}(\boldsymbol{x})}(\boldsymbol{g})$ of $\boldsymbol{G}(\boldsymbol{x})$ writes

$$p_{\boldsymbol{G}(\boldsymbol{x})}(\boldsymbol{g}) = c \exp\left(- < [\Lambda_{\boldsymbol{x}}], \exp\left(\sum_{i=1}^{N} g_i [E_i]\right) > -\lambda_{\boldsymbol{x}} \sum_{i=1}^{N} g_i \mathrm{tr}([E_i])\right)\,, \tag{12}$$

where $[\Lambda_{\boldsymbol{x}}]$ and $\lambda_{\boldsymbol{x}}$ are the Lagrange multipliers such that the constraints respectively defined by Eq. (9) and Eq. (10) are satisfied.

3 Random generation algorithms

Let $\left\{\{\xi^\ell(\boldsymbol{x}), \boldsymbol{x} \in \mathbb{R}^d\}\right\}_{\ell=1}^{\ell=n(n+1)/2}$ and $\left\{\{\Xi^{\ell'}(\boldsymbol{x}), \boldsymbol{x} \in \mathbb{R}^d\}\right\}_{\ell'=1}^{\ell'=N}$ be two sets of independent second-order centered homogeneous real-valued Gaussian random fields, defined on a probability space $(\Theta, \mathcal{T}, P)$ and indexed by $\mathbb{R}^d$, such that for all $\boldsymbol{x}$ in $\mathbb{R}^d$, $\mathbb{E}\{\xi^\ell(\boldsymbol{x})^2\} = 1$ and $\mathbb{E}\{\Xi^{\ell'}(\boldsymbol{x})^2\} = 1$. These sets of Gaussian random fields are completely defined by the associated sets $\{\mathrm{R}_{\xi^\ell}\}_{\ell=1}^{\ell=n(n+1)/2}$ and $\{\mathrm{R}_{\Xi^{\ell'}}\}_{\ell'=1}^{\ell'=N}$ of normalized autocorrelation functions (which are assumed to be continuous hereinafter, hence implying the mean-square continuity for the associated random fields). Let $\{\boldsymbol{\xi}(\boldsymbol{x}), \boldsymbol{x} \in \mathbb{R}^d\}$ and $\{\boldsymbol{\Xi}(\boldsymbol{x}), \boldsymbol{x} \in \mathbb{R}^d\}$ be the $\mathbb{R}^{n(n+1)/2}$-valued and $\mathbb{R}^N$-valued Gaussian random fields such that for all $\boldsymbol{x}$ in Ω, $\boldsymbol{\xi}(\boldsymbol{x}) = (\xi^1(\boldsymbol{x}), \ldots, \xi^{n(n+1)/2}(\boldsymbol{x}))$ and $\boldsymbol{\Xi}(\boldsymbol{x}) = (\Xi^1(\boldsymbol{x}), \ldots, \Xi^N(\boldsymbol{x}))$.

3.1 Random generator for random field $\{[\boldsymbol{A}(\boldsymbol{x})], \boldsymbol{x} \in \Omega\}$

Following [17], the random variable $[\boldsymbol{A}(\boldsymbol{x})]$ whose p.d.f. is defined by Eq. (5) can be decomposed as

$$\forall \boldsymbol{x} \in \Omega\,, \quad [\boldsymbol{A}(\boldsymbol{x})] = [\underline{L}(\boldsymbol{x})]^{\mathrm{T}}[\boldsymbol{H}(\boldsymbol{x})]^{\mathrm{T}}[\boldsymbol{H}(\boldsymbol{x})]\,[\underline{L}(\boldsymbol{x})]\,, \tag{13}$$

where $[\underline{L}(\boldsymbol{x})]$ is such that $[\underline{A}(\boldsymbol{x})] = [\underline{L}(\boldsymbol{x})]^{\mathrm{T}}\,[\underline{L}(\boldsymbol{x})]$ (see section 2.3.1) and $[\boldsymbol{H}(\boldsymbol{x})]$ is an upper-triangular $\mathbb{M}_n(\mathbb{R})$-valued random matrix whose elements are defined, for $1 \leq i \leq j \leq n$, as:

$$[H(\boldsymbol{x})]_{ij} = \begin{cases} \delta(\boldsymbol{x})\,\xi^{\alpha_{ij}}(\boldsymbol{x})/(n+1)^{1/2} & \text{if} \quad i < j \\ \delta(\boldsymbol{x})\left(2\mathrm{F}^{-1}_{\mathcal{G}(\beta_j(\boldsymbol{x}),1)}(\mathrm{F}_{\mathcal{N}}(\xi^{\alpha_{jj}}(\boldsymbol{x})))/(n+1)\right)^{1/2} & \text{if} \quad i = j \end{cases}\,, \tag{14}$$

in which

$$\alpha_{ij} = i + j(j-1)/2 \tag{15}$$

and

$$\beta_j(\boldsymbol{x}) = (n+1)/(2\delta(\boldsymbol{x})^2) + (1-j)/2\,. \tag{16}$$

In Eq. (14), $\mathrm{F}^{-1}_{\mathcal{G}(\beta_j(\boldsymbol{x}),1)}$ and $\mathrm{F}_{\mathcal{N}}$ are the Gamma inverse cumulative distribution function (with parameters $\beta_j(\boldsymbol{x})$ and 1) and the standard normal cumulative distribution function, respectively.

3.2 Random generator for random field $\{[\boldsymbol{G}(\boldsymbol{x})], \boldsymbol{x} \in \Omega\}$

In order to construct an efficient random generator for random field $\{\boldsymbol{G}(\boldsymbol{x}), \boldsymbol{x} \in \Omega\}$ [7], we introduce a $\mathbb{R}^N$-valued centered second-order Gaussian random field $\boldsymbol{W} = \{\boldsymbol{W}_{\boldsymbol{x}}(r) = (W^{(1)}_{\boldsymbol{x}}(r), \ldots, W^{(N)}_{\boldsymbol{x}}(r)),\ \boldsymbol{x} \in \Omega,\ r \in \mathbb{R}^+\}$ such that for all $\boldsymbol{x}$ in Ω, $\boldsymbol{W}_{\boldsymbol{x}}(0) = \boldsymbol{0}$ a.s. and such that the generalized r-derivative of $\boldsymbol{W}$ is the cylindrical normalized Gaussian white noise $\boldsymbol{B}$ [11]. The covariance function $[\mathrm{C}_{\boldsymbol{B}}]$ of the latter is further defined as

$$\forall (\boldsymbol{x}, \boldsymbol{x}') \in \Omega \times \Omega, \quad \forall \tau \in \mathbb{R}, \quad [\mathrm{C}_{\boldsymbol{B}}(\boldsymbol{x}, \boldsymbol{x}', t+\tau, t)] = \delta_0(\tau)[\mathrm{R}_{\boldsymbol{B}}(\boldsymbol{x}, \boldsymbol{x}')]\,, \tag{17}$$

where δ_0 the Dirac generalized function concentrated at the origin of $\mathbb{R}$ and $[\mathrm{R}_{\boldsymbol{B}}] : \Omega \times \Omega \to \mathbb{M}_N(\mathbb{R})$ is the continuous function given by

$$\forall\ 1 \leqslant \ell, \ell' \leqslant N, \quad [\mathrm{R}_{\boldsymbol{B}}(\boldsymbol{x}, \boldsymbol{x}')]_{\ell\ell'} := \delta_{\ell\ell'}\mathrm{R}_{\underline{\Xi}^{\ell'}}(\boldsymbol{x} - \boldsymbol{x}')\,, \tag{18}$$

with $\delta_{\ell\ell'}$ is the Kronecker delta. It follows that for any $\boldsymbol{x}$ fixed in Ω, the stochastic process $\boldsymbol{W}_{\boldsymbol{x}} = \{\boldsymbol{W}_{\boldsymbol{x}}(r), r \geq 0\}$ is a normalized $\mathbb{R}^N$-valued Wiener process.

Let $[\Lambda_{\boldsymbol{x}}] = \sum_{i=1}^N \lambda^{(i)}_{\boldsymbol{x}}[E_i]$ and let $\boldsymbol{\lambda}_{\boldsymbol{x}} = (\lambda^{(1)}_{\boldsymbol{x}}, \ldots, \lambda^{(N)}_{\boldsymbol{x}}, \lambda_{\boldsymbol{x}})$. We denote by Φ the potential function defined from $\mathbb{R}^N$ into $\mathbb{R}$ by

$$\Phi(\boldsymbol{u}; \boldsymbol{\lambda}_{\boldsymbol{x}}) = \ll \sum_{i=1}^N \lambda^{(i)}_{\boldsymbol{x}}[E_i], \exp\left(\sum_{i=1}^N u_i[E_i]\right) \gg + \lambda_{\boldsymbol{x}} \sum_{i=1}^N u_i\ \mathrm{tr}([E_i]) \tag{19}$$

and such that (see Eq. (12))

$$\forall \boldsymbol{g} \in \mathbb{R}^N, \quad p_{\boldsymbol{G}(\boldsymbol{x})}(\boldsymbol{g};\ \boldsymbol{x}) = c\ \exp\left(-\Phi(\boldsymbol{g};\boldsymbol{\lambda}_{\boldsymbol{x}})\right)\ . \tag{20}$$

For all $\boldsymbol{x}$ fixed in Ω, we introduce the $\mathbb{R}^N \times \mathbb{R}^N$-valued Markov stochastic process $\{(\boldsymbol{U}_{\boldsymbol{x}}(r), \boldsymbol{V}_{\boldsymbol{x}}(r)), r \in \mathbb{R}^+\}$, defined on probability space $(\Theta, \mathcal{T}, \mathcal{P})$, satisfying the following Itô stochastic differential equation (ISDE),

$$\forall r \in \mathbb{R}^+, \left\{ \begin{array}{l} \mathrm{d}\boldsymbol{U}_{\boldsymbol{x}}(r) = \boldsymbol{V}_{\boldsymbol{x}}(r)\mathrm{d}r \\ \mathrm{d}\boldsymbol{V}_{\boldsymbol{x}}(r) = -\nabla_{\boldsymbol{u}}\Phi(\boldsymbol{U}_{\boldsymbol{x}}(r);\boldsymbol{\lambda}_{\boldsymbol{x}})\mathrm{d}r - \dfrac{f^0_{\boldsymbol{x}}}{2}\boldsymbol{V}_{\boldsymbol{x}}(r)\mathrm{d}r + \sqrt{f^0_{\boldsymbol{x}}}\mathrm{d}\boldsymbol{W}_{\boldsymbol{x}}(r) \end{array} \right. , \tag{21}$$

supplemented by the following initial conditions:

$$\boldsymbol{U}_{\boldsymbol{x}}(0) = \boldsymbol{U}^0_{\boldsymbol{x}}\ , \quad \boldsymbol{V}_{\boldsymbol{x}}(0) = \boldsymbol{V}^0_{\boldsymbol{x}}\ \text{a.s.}\ , \tag{22}$$

where the probability distribution of $(\boldsymbol{U}^0_{\boldsymbol{x}}, \boldsymbol{V}^0_{\boldsymbol{x}})$ is arbitrary and independent of the stochastic process $\{\boldsymbol{W}_{\boldsymbol{x}}(r), r \geq 0\}$ (deterministic initial conditions can be retained). In Eq. (21), $\{f^0_{\boldsymbol{x}}\}_{\boldsymbol{x}\in\Omega}$ denotes a family of free $\mathbb{R}^+$-valued parameters that can be calibrated in order to shorten the transient regime while solving the ISDE. Provided that the potential function Φ satisfies a set of fundamental properties (see [18] and the references therein), it can be shown that the above stochastic differential equation admits a unique second-order stationary solution and that

$$\lim_{r\to+\infty} \boldsymbol{U}_{\boldsymbol{x}}(r) = \boldsymbol{G}(\boldsymbol{x}) \tag{23}$$

for the convergence in probability distribution. In this work, the ISDE is discretized by using an explicit Störmer-Verlet algorithm [2–8–23], in which the Gaussian increment of Wiener process $\boldsymbol{W}_{\boldsymbol{x}}$ between instants r_k and r_{k+1} is defined, in view of Eqs. (17–18), as

$$\Delta\boldsymbol{W}^{k+1}_{\boldsymbol{x}} = \boldsymbol{W}_{\boldsymbol{x}}(r_{k+1}) - \boldsymbol{W}_{\boldsymbol{x}}(r_k) = \sqrt{\Delta r}\ \boldsymbol{\Xi}^{k+1}(\boldsymbol{x}) \quad \forall k \geqslant 1\ , \tag{24}$$

with $\Delta r = r_{k+1} - r_k$ the time step and $\boldsymbol{\Xi}^{k+1}(\boldsymbol{x})$ the $(k+1)$-th independent copy of random variable $\boldsymbol{\Xi}(\boldsymbol{x})$.

4 Numerical application

4.1 Problem statement

Below, the proposed model is used so as to represent the random field of apparent properties obtained from the two-dimensional stochastic homogenization of a porous material with random interphases. In order to keep the presentation as simple as possible, the application is voluntarily restricted to the random matrix case (that is, the calibration is performed on the first-order probability distribution only) and reference to spatial indexation is therefore dropped from now on. Note that a discussion regarding the identification of a target correlation structure can be found in [7].

A square domain Ω of length 6 *mm* is considered. This domain is occupied by an isotropic matrix and randomly filled with pores of constant diameter $d = 1.1$ *mm*. The underlying random generator is a simple

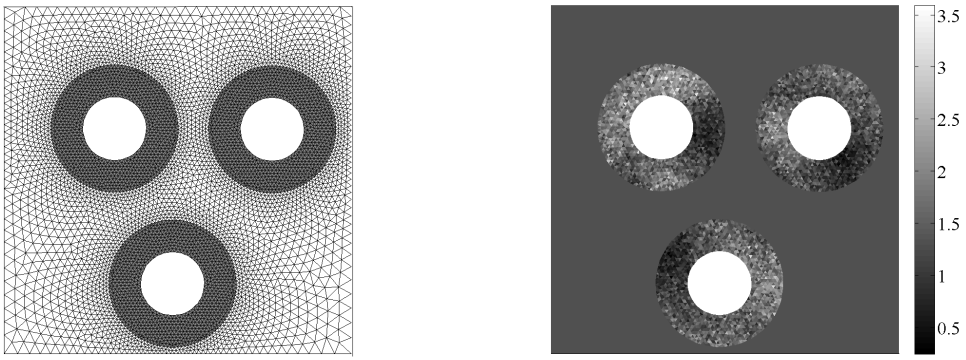

Figure 1: One realization of the random porous material in meshed view (left) and associated random field $\{C_{11}(\boldsymbol{x}), \boldsymbol{x} \in \Omega\}$ in *GPa* (right).

uniform generator for non-overlapping pores. The porosity (i.e. the ratio between the surface fraction of pores and the surface of Ω) is set to 0.1 and does not change from one realization to another. In addition, we define, for each pore, an interphase region of constant thickness $h = d/2$, where the elastic properties are allowed to fluctuate randomly from point to point. Figure 1 (left) shows one realization of the random material in a meshed view, where the regions corresponding to random interphases appear in grey.

The values of Young's modulus and Poisson ratio for the matrix phase are set to 1.1 *GPa* and 0.25, respectively, whereas the elastic properties of each interphase are defined by a random field model (note that independent realizations are used for all the interphases). For illustration purposes, it is assumed that the elasticity tensor random field associated with the interphase region belongs to the class SFE^+ of random fields introduced in sections 2.3.1 and 3.1 and defined in [17], for which:

- The mean model coincides with the matrix elasticity tensor.
- The associated dispersion field (see Eq. (7)), denoted by $\boldsymbol{x} \mapsto \delta_{\mathrm{database}}(\boldsymbol{x})$, is homogeneous and such that $\delta_{\mathrm{database}}(\boldsymbol{x}) = 0.5$ at any point $\boldsymbol{x}$ in the interphase region.
- The correlation functions associated with the underlying second-order homogeneous real-valued Gaussian random fields (see [17] for details) are assumed to be the same regardless of the random field under consideration, and are writen in a separable polar form. Furthermore, the orthoradial correlation function satisfies additional properties related to the axisymmetry of the interphase region, such as 2π-periodicity and even parity with respect to the angular lag. The values of the radial and orthoradial spatial correlation lengths of all the Gaussian random fields are finally set to h and π, respectively.

From a physical point of view, the interphase is therefore viewed as a local random perturbation of the surrounding matrix phase. As an illustration, one realization of random field $\{C_{11}(\boldsymbol{x}), \boldsymbol{x} \in \Omega\}$ is displayed in Fig. 1 (right).

For each realization of the random medium, the linear homogenization problem is solved by the finite element method under kinematic uniform (Dirichlet) boundary conditions. In practice, the domain Ω successively undergoes three load cases of the following form:

$$\forall \boldsymbol{x} \in \partial\Omega,\ \boldsymbol{u}(\boldsymbol{x}) = [\overline{E}]\boldsymbol{x}, \tag{25}$$

where $\partial\Omega$ is the boundary of Ω and the so-called macroscopic strain tensor $[\overline{E}]$ is equal either to $\boldsymbol{e}^1\otimes\boldsymbol{e}^1$, $\boldsymbol{e}^2\otimes\boldsymbol{e}^2$ or to $(\boldsymbol{e}^1\otimes\boldsymbol{e}^2+\boldsymbol{e}^2\otimes\boldsymbol{e}^1)/2$, with $\boldsymbol{e}^1=(1,0)$ and $\boldsymbol{e}^2=(0,1)$. The apparent elasticity matrix is subsequently obtained through spatial averaging by invoking the superposition principle (see [25] for instance).

4.2 Matrix basis and projection operator

From a modeling point of view, the material symmetry exhibited by the homogenized elasticity matrix is expected to be close to isotropy. Therefore, one has $\mathbb{M}_3^{\mathrm{sym}}(\mathbb{R}) = \mathrm{span}\{[E_1],[E_2]\}$, where the matrix basis is defined as

$$[E_1] = \begin{pmatrix} 1/2 & 1/2 & 0 \\ 1/2 & 1/2 & 0 \\ 0 & 0 & 0 \end{pmatrix} \tag{26}$$

and

$$[E_2] = \begin{pmatrix} 1/2 & -1/2 & 0 \\ -1/2 & 1/2 & 0 \\ 0 & 0 & 1 \end{pmatrix}. \tag{27}$$

The above basis satisfies the usual properties: $[E_1]^2=[E_1]$, $[E_2]^2=[E_2]$, $[E_1]\,[E_2]=[E_2]\,[E_1]=[0_3]$ and $[E_1]+[E_2]=[I_3]$. Any matrix $[C]\in\mathbb{M}_3^{\mathrm{sym}}(\mathbb{R})$ can then be written as $[C]=a_1[E_1]+a_2[E_2]$, with $a_1>0$ and $a_2>0$. Furthermore, the projection $[C^{\mathrm{sym}}]$ of any symmetric positive-definite matrix $[C]$ onto $\mathbb{M}_3^{\mathrm{sym}}(\mathbb{R})$ (in the sense of the Euclidean projection) can be classically defined through a projection operator P^{sym} such that

$$[C^{\mathrm{sym}}] = [P^{\mathrm{sym}}([C])] = a_1^{\mathrm{sym}}\,[E_1] + a_2^{\mathrm{sym}}\,[E_2]\,, \tag{28}$$

where the two coefficients of the projection are easily found by minimizing the Euclidean distance between $[C]$ and $[C^{\mathrm{sym}}]$:

$$a_1^{\mathrm{sym}} = (C_{11}+2C_{12}+C_{22})/2\,,\quad a_2^{\mathrm{sym}} = (C_{11}-2C_{12}+C_{22}+2C_{33})/4\,. \tag{29}$$

4.3 Potential function and MaxEnt constraints associated with random matrix $[\boldsymbol{G}]$

Since the two matrices $[E_1]$ and $[E_2]$ defined by Eqs. (26) and (27) are two commutating projectors, the potential function defined by Eq. (19) can be written as

$$\Phi(g_1,g_2) = \lambda_1\exp\{g_1\} + \lambda g_1 + 2\left(\lambda_2\exp\{g_2\}+\lambda g_2\right)\,, \tag{30}$$

where $\lambda_1 > 0$, $\lambda_2 > 0$ and $\lambda < 0$ in order to make the associated p.d.f. (defined by Eqs. (20–30)) integrable. Eq. (30) shows that the two-dimensional ISDE reduces to two uncoupled one-dimensional ones, and that G_1 and G_2 are statistically independent random variables. This latter result is consistent with other results about the statistical dependence of elastic moduli available in the literature (see [6]). The MaxEnt constraints further read as

$$\mathbb{E}\{\exp\{g_1\}\} = 1 \,, \tag{31}$$

$$\mathbb{E}\{\exp\{g_2\}\} = 1 \tag{32}$$

and

$$\mathbb{E}\{g_1\} + 2\mathbb{E}\{g_2\} = \nu \,. \tag{33}$$

Note that the above equations, together with Jensen's inequality, show that for the isotropic case, parameter ν is such that $\nu \leqslant 0$.

The identification of the Lagrange multipliers can be performed, either by enforcing Eqs. (31), (32) and (33) to hold (should the value of parameter ν be known or imposed), or by solving a statistical inverse problem. In both cases, solving the associated optimization problem may be challenging (since the Lagrange multipliers belong to semi-bounded parts of $\mathbb{R}$) and requires a good initial guess $\boldsymbol{\lambda}^0 = (\lambda_1^0, \lambda_2^0, \lambda^0)$ to be proposed. To this aim, note first that a Gaussian approximation can be readily obtained, for moderate levels of statistical fluctuations, by using a second-order Taylor expansion of the exponential terms in Eq. 30. Substituting this approximation into Eqs. (31), (32) and (33) and noticing that $-\lambda/\lambda_1 \simeq 1$ and $-\lambda/\lambda_2 \simeq 1$ for small levels of fluctuations, it can be deduced that a good initial guess can be obtained as:

$$\lambda_1^0 = -\lambda^0 \,, \quad \lambda_2^0 = -\lambda^0 \,, \quad \lambda^0 = \frac{3\nu + 4 + \sqrt{\nu^2 + 16}}{8\nu} \,. \tag{34}$$

When $\nu \uparrow 0$, one has $\lambda^0 \to -\infty$ and then $\lambda_1^0 \to +\infty$ and $\lambda_2^0 \to +\infty$, so that the probability distribution $P_{G_1}(\mathrm{d}g_1)$ (resp. $P_{G_2}(\mathrm{d}g_2)$) associated with random variable G_1 (resp. G_2) tends to the measure $\delta_0(g)$ (which is the Dirac measure at the origin of $\mathbb{R}$) and $\exp\{[\boldsymbol{G}]\} \to [I_3]$ in probability. Consequently, parameter λ allows the level of statistical fluctuations of the $\mathbb{M}_3^{\mathrm{sym}}(\mathbb{R})$-valued part of the model to be controlled.

4.4 Identification procedure

Let $[C^{\mathrm{exp}}(\theta_1)], \ldots, [C^{\mathrm{exp}}(\theta_{N^{\mathrm{exp}}})]$ be a set of N^{exp} experimental realizations of the apparent tensor $[\boldsymbol{C}]$ obtained from stochastic homogenization (under Dirichlet boundary conditions) of N^{exp} realizations of the random medium occupying domain Ω – the experimental realizations being then understood as the simulated ones hereinafter. Below, we denote by $\boldsymbol{C}$ the $\mathbb{V}$-valued vector representation of any elasticity matrix $[\boldsymbol{C}]$ defined with respect to the usual vec-operator, with $\mathbb{V}$ a given subset of $\mathbb{R}^{n(n+1)/2}$. Accordingly, we denote by $\boldsymbol{c}^{\mathrm{exp}}(\theta_1), \ldots, \boldsymbol{c}^{\mathrm{exp}}(\theta_{N^{\mathrm{exp}}})$ the aforementionned set of realizations.

From Eqs. (3), (5) and (12), it is seen that the p.d.f. $p_{\boldsymbol{C}}$ of $\boldsymbol{C}$ depends on the parameter δ associated with the anisotropic germ (note that this parameter does not have to be confused with the parameter $\delta_{\mathrm{database}}$ used for generating the database; see section 4.1), as well as on the mean value $[\underline{C}]$ and vector-valued Lagrange

multiplier $\boldsymbol{\lambda} = (\lambda_1, \lambda_2, \lambda)$ (associated with the germ with values in $\mathbb{M}_3^{\mathrm{sym}}(\mathbb{R})$). We therefore write the above p.d.f. as $p_{\boldsymbol{C}}(\cdot; \delta, \boldsymbol{\lambda}, [\underline{C}])$.

An optimal set of model parameters can be identified by using the maximum likelihood method, that is, by solving the following optimization problem:

$$(\delta^{\mathrm{opt}}, \boldsymbol{\lambda}^{\mathrm{opt}}, [\underline{C}^{\mathrm{opt}}]) = \mathrm{argmax}_{\mathbb{S}}\ \mathcal{L}(\delta, \boldsymbol{\lambda}, [\underline{C}]) \tag{35}$$

where $\mathbb{S}$ is the admissible set defined as

$$\mathbb{S} =]0,\ \sqrt{(n+1)/(n+5)}[\ \times\ \mathbb{H}\ \times\ \mathbb{M}_n^+(\mathbb{R}) \tag{36}$$

and $\mathcal{L}$ is the so-called likelihood function given by:

$$\mathcal{L}(\delta, \boldsymbol{\lambda}, [\underline{C}]) = \prod_{i=1}^{N^{\mathrm{exp}}} p_{\boldsymbol{C}}(\boldsymbol{c}^{exp}(\theta_i); \delta, \boldsymbol{\lambda}, [\underline{C}])\ . \tag{37}$$

Note that for numerical convenience, one may equivalently chose to maximise the log-likelihood function defined as the natural logarithm of $\mathcal{L}$. In practice, the estimation of the joint p.d.f. $p_{\boldsymbol{C}}$ can be performed by having recourse to a multidimensional kernel estimator. Since the latter may not perform well, depending on the shape of the p.d.f., one may also consider working on marginal p.d.f. only and solving an optimization problem where the likelihood function is defined as:

$$\widetilde{\mathcal{L}}(\delta, \boldsymbol{\lambda}, [\underline{C}]) = \prod_{i=1}^{N^{\mathrm{exp}}} \prod_{j=1}^{n(n+1)/2} p_{\boldsymbol{C}_j}(\boldsymbol{c}_j^{exp}(\theta_i); \delta, \boldsymbol{\lambda}, [\underline{C}])\ . \tag{38}$$

One should note that the above optimization problems have to be solved in part on the positive-definite cone, which may require the use of specific semidefinite programming algorithms. When the value of N^{exp} is large enough to allow for the use of converged statistical estimators, the mean value $[\underline{C}^{\mathrm{opt}}]$ may be simply approximated by the empirical mean $[\widehat{\underline{C}}]$, namely

$$[\underline{C}^{\mathrm{opt}}] \simeq [\widehat{\underline{C}}] = (1/N^{\mathrm{exp}}) \sum_{i=1}^{N^{\mathrm{exp}}} [C^{exp}(\theta_i)]\ . \tag{39}$$

Concerning the identification of the remaining parameters, there is no way to use statistical estimators to compute either δ^{opt} or ν (which could provide a good guess for $\boldsymbol{\lambda}^{\mathrm{opt}}$ through Eq. (34)), because the multiplicative definition given by Eq. (3) prevents from getting independent realizations of $[\boldsymbol{A}]$ and $[\boldsymbol{M}]$. Whereas the computation of δ^{opt} may not critically rely on a good starting value, since this parameter belongs to an open bounded domain of $\mathbb{R}$ (see Eq. (36)), the estimation of an efficient prior guess $\boldsymbol{\lambda}^0$ for $\boldsymbol{\lambda}^{\mathrm{opt}}$ is of particular interest in order to reduce the computation time. Following the discussion provided in section 4.2, it is seen

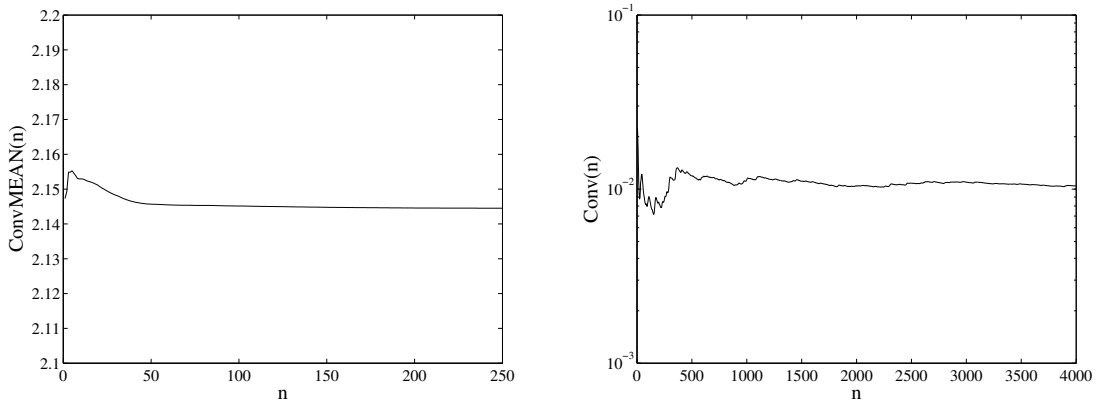

Figure 2: Left: graph of $n \mapsto \text{ConvMEAN}(n)$. Right: graph of $n \mapsto \text{Conv}(n)$ for an arbitrary value of Lagrange multipliers λ_1, λ_2 and λ.

that $\boldsymbol{\lambda}^0$ may be defined by extracting the isotropic part from the experimental realizations and by substituting the following statistical estimator

$$\widehat{\nu} = \frac{1}{N^{\text{exp}}} \sum_{i=1}^{N^{\text{exp}}} \log\left(\det\left([\underline{C}^{\text{opt}}]^{-1/2}\ P^{\text{sym}}([C^{exp}(\theta_i)])\ [\underline{C}^{\text{opt}}]^{-1/2}\right)\right) . \tag{40}$$

for parameter ν in Eq. (34).

4.5 Numerical results

In this application, $N^{\text{exp}} = 250$ experimental realizations are considered. The mean of the elasticity tensor is first computed as (in *GPa*)

$$[\widehat{\underline{C}}] = \begin{pmatrix} 1.2848 & 0.4281 & 0.0016 \\ 0.4281 & 1.3229 & -0.0006 \\ 0.0016 & -0.0006 & 0.9123 \end{pmatrix} , \tag{41}$$

hence providing, through a projection onto $\mathbb{M}_3^{\text{sym}}(\mathbb{R})$, the following value of $[\underline{C}^{\text{sym}}] = P^{\text{sym}}([\underline{C}^{\text{opt}}])$:

$$[\underline{C}^{\text{sym}}] = \begin{pmatrix} 1.3130 & 0.4189 & 0 \\ 0.4189 & 1.3130 & 0 \\ 0 & 0 & 0.8941 \end{pmatrix} . \tag{42}$$

The convergence of the estimator for the mean value is characterized by the convergenve of mapping $n \mapsto \text{ConvMEAN}(n) = \|(1/n)\sum_{i=1}^{n}[C^{\text{exp}}(\theta_i)]\|_{\text{F}}$, the graph of which is shown in Fig. 2 (left). The distance between $[\widehat{\underline{C}}]$ and its isotropic projection, defined as $\|[\widehat{\underline{C}}] - P^{\text{sym}}([\widehat{\underline{C}}])\|_{\text{F}}$, is equal to 3.7×10^{-2}, showing that the apparent

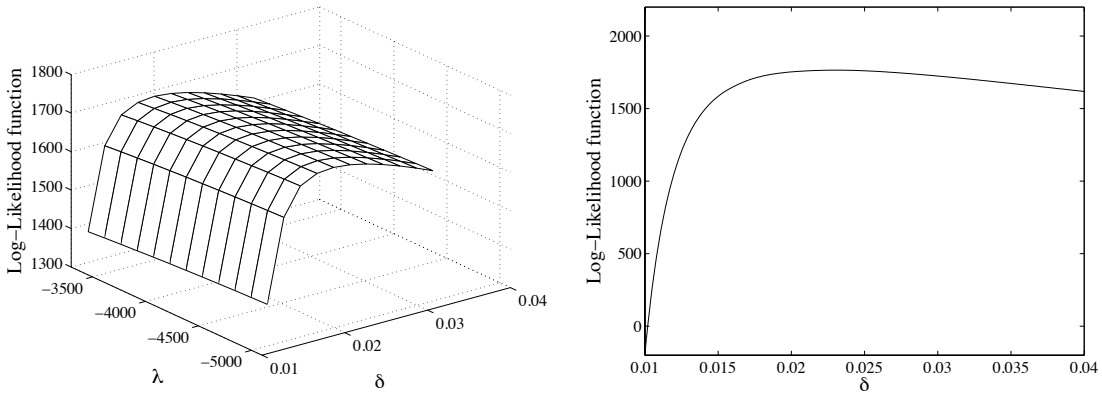

Figure 3: Left: graph of the log-likelihood function $(\delta, \lambda) \mapsto \ln\left(\widetilde{\mathcal{L}}(\delta, (-\lambda, -\lambda, \lambda), [\underline{C}^{\text{opt}}])\right)$. Right: graph of the log-likelihood function $\delta \mapsto \ln\left(\widetilde{\mathcal{L}}(\delta, (+\infty, +\infty, -\infty), [\underline{C}^{\text{opt}}])\right)$.

elasticity matrix is approximately isotropic in mean. One should note that such a convergence with respect to the isotropy class reflects the level of convergence towards the effective properties, as suggested by the rather small level of statistical fluctuations exhibited by the apparent matrix (with a coefficient of variation of about 2.2%) and as discussed elsewhere in the literature (see [13] for instance).

Concerning the random generation in $\mathbb{M}_3^{\text{sym}}(\mathbb{R})$, the ISDE defined by Eq. (21) (in which $f^0 = 500$) is discretized with $\Delta r = 0.01$. The convergence towards the stationary solution is investigated through the convergence of mapping $n \mapsto \text{Conv}(n) = (1/n) \sum_{i=1}^{n} \|\boldsymbol{U}((i-1)\Delta r)\|^2$ (which shows the convergence of the ergodic estimator for the second-order moment of random variable $\boldsymbol{U}$). The graph of $n \mapsto \text{Conv}(n)$ is displayed in Fig. 2 for arbitrary values of the Lagrange multipliers, and it is seen that the stationary solution is reached after 3 000 iterations. Note that this convergence must be checked for any value of Lagrange multiplier $\boldsymbol{\lambda}$. The plot of the log-likelihood function $(\delta, \lambda) \mapsto \ln\left(\widetilde{\mathcal{L}}(\delta, (-\lambda, -\lambda, \lambda), [\underline{C}^{\text{opt}}])\right)$ is shown in Fig. 3, where the range of parameter λ has been inferred by using the Gaussian approximation and Eq. (34). It is observed that the log-likelihood function monotonically increases as λ tends to $-\infty$, regardless of the current value of parameter δ. This behavior tends to suggest that the anisotropic part is predominant compared to the fluctuations in $\mathbb{M}_3^{\text{sym}}(\mathbb{R})$, so that an optimal solution may be sought by setting $\lambda \to -\infty$ (that is, for $[\boldsymbol{M}] \to [\underline{C}^{\text{sym}}]$). The graph of the log-likelihood function $\delta \mapsto \ln\left(\widetilde{\mathcal{L}}(\delta, (+\infty, +\infty, -\infty), [\underline{C}^{\text{opt}}])\right)$ is shown in Fig. 3 (right), where it is seen that the maximum, reached for $\delta^{\text{opt}} = 0.0231$, is higher than the maximum obtained while optimizing on both δ and λ. This fact confirms the relevance of the identification strategy. Finally, the probability density functions of the data are compared with the ones obtained by Monte Carlo simulations (in which the above optimal parameters are used) for all the components of the random elasticity matrix. These p.d.f. are displayed in Figs 4, 5 and 6, where the p.d.f. for the simulated data have been obtained from 5 000 independent realizations. A fairly good agreement is observed, although the number of experimental realizations is too small in order to obtain converged kernel estimators.

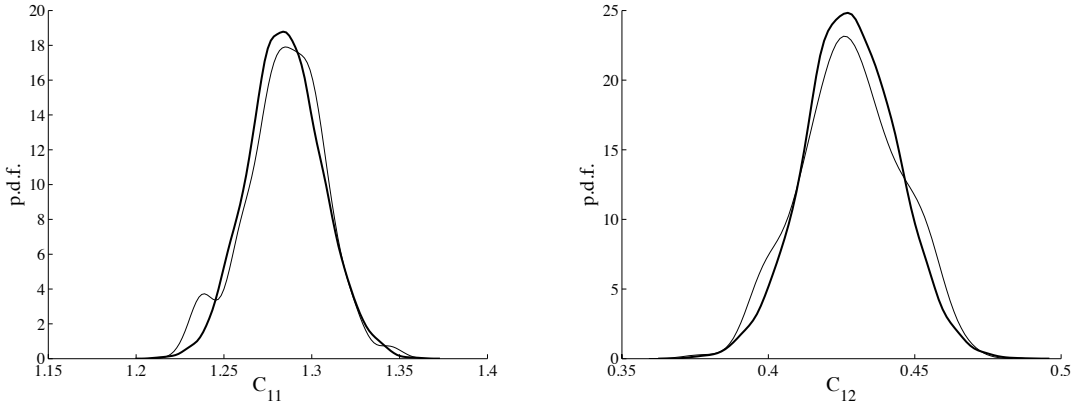

Figure 4: Graphs of the probability density functions of C_{11} (left) and C_{12} (right): experimental data (thin line) and simulated data (thick line).

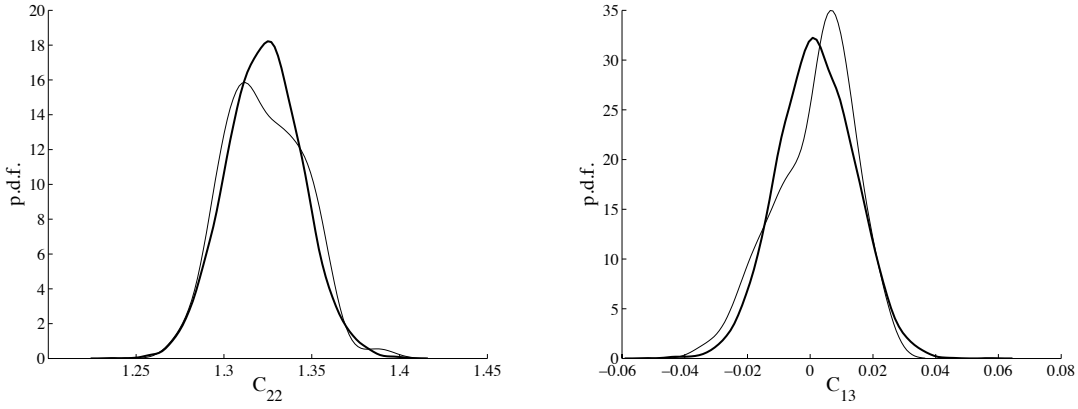

Figure 5: Graphs of the probability density functions of C_{22} (left) and C_{13} (right): experimental data (thin line) and simulated data (thick line).

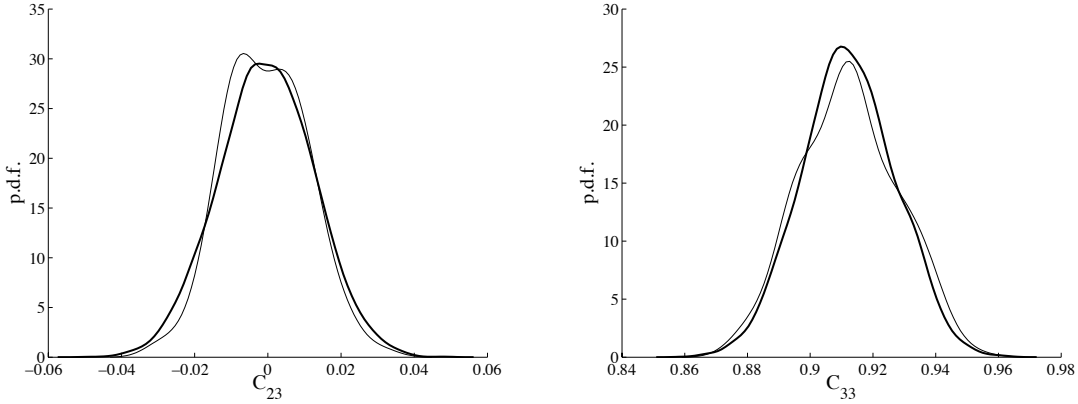

Figure 6: Graphs of the probability density functions of C_{23} (left) and C_{33} (right): experimental data (thin line) and simulated data (thick line).

5 Conclusion

In this paper, we addressed the modeling of randomness in multiscale analysis of heterogeneous materials through the construction of probabilistic models for matrix-valued non-Gaussian random fields. A general framework relying on the use of the maximum entropy principle is introduced. As an example, a prior algebraic probabilistic model for random fields exhibiting some symmetry propertries, recently proposed in the literature, is discussed keeping all mathematical details at their most basic level. Random generators adapted to the Monte Carlo simulation of the proposed generalized representation are provided. Finally, the identification strategy is proposed and exemplified through the modeling of the random linear elastic properties exhibited by a porous microstructure containing stochastic heterogeneous interphases. It is shown that the model successfully allows for the stochastic modeling of the random elasticity matrix (taking into account all the statistical dependencies between its components), hence providing a path towards its use in theoretical and experimental analysis of complex materials.

References

[1] Clément, A., Soize, C., Yvonnet, J.: Computational nonlinear stochastic homogenization using a non-concurrent multiscale approach for hyperelastic heterogeneous microstructures analysis. International Journal of Numerical Methods in Engineering **91**, 799–824 (2012)

[2] De Vogelaere, R.: Methods of integration which preserve the contact transformation property of the hamiltonian equations. Technical Report 4, University of Notre Dame (1956)

[3] Guilleminot, J., Noshadravan, A., Soize, C., Ghanem, R. G.: A probabilistic model for bounded elasticity tensor random fields with application to polycrystalline microstructures. Computer Methods in Applied

Mechanics and Engineering **200**, 1637–1648 (2011)
[4] Guilleminot, J., Soize, C.: Non-Gaussian positive-definite matrix-valued random fields with constrained eigenvalues: Application to random elasticity tensors with uncertain material symmetries. International Journal of Numerical Methods in Engineering **88**, 1128–1151 (2011)
[5] Guilleminot, J., Soize, C.: Stochastic modeling of anisotropy in multiscale analysis of heterogeneous materials: a comprehensive overview on random matrix approaches. Mechanics of Materials **44**:35–46 (2012)
[6] Guilleminot, J., Soize, C.: On the Statistical Dependence for the Components of Random Elasticity Tensors Exhibiting Material Symmetry Properties. Journal of Elasticity **111**, 109–130 (2013)
[7] Guilleminot, J., Soize, C.: Stochastic model and generator for random fields with symmetry properties: Application to the mesoscopic modeling of elastic random media. SIAM Multiscale Modeling and Simulation, **11**, 840–870 (2013)
[8] Hairer, E., Lubich, C., Wanner, G.: Geometric Numerical Integration. Structure-Preserving Algorithms for Ordinary Differential Equations. Springer, Berlin (2002)
[9] Jaynes, E. T.: Information theory and statistical mechanics. Phys. Rev. **106**(4), 620–630 (1957)
[10] Jaynes, E. T.: Information theory and statistical mechanics. Phys. Rev. **108**(2), 171–190 (1957)
[11] Kree, P., Soize, C.: Mathematics of Random Phenomena. Reidel Publishing Company, Dordrecht, Holland (1986)
[12] Ostoja-Starzewski, M.: Microstructural Randomness and Scaling in Mechanics of Materials. Chapman and Hall-CRC (2008)
[13] Salmi, M., Auslender, F., Bornert, M., Fogli, M.: Various estimates of Representative Volume Element sizes based on a statistical analysis of the apparent behavior of random linear composites. C. R. Mecanique **340**, 230–246 (2012)
[14] Serra, J.: Image analysis and Mathematical Morphology. Academic Press, London (1982)
[15] Shannon, C. E.: A mathematical theory of communication. Bell System Technical Journal **27**, 379–423/623–659 (1948)
[16] Soize, C.: A non parametric model of random uncertainties on reduced matrix model in structural dynamics. Probabilistic Engineering Mechanics **15**(3), 277–294 (2000)
[17] Soize, C.: Non-gaussian positive-definite matrix-valued random fields for elliptic stochastic partial differential operators. Computer Methods in Applied Mechanics and Engineering **195**, 26–64 (2006)
[18] Soize, C.: Construction of probability distributions in high dimension using the maximum entropy principle: Applications to stochastic processes, random fields and random matrices. International Journal of Numerical Methods in Engineering **76**, 1583–1611 (2008)
[19] Soize, C.: Tensor-valued random fields for meso-scale stochastic model of anisotropic elastic microstructure and probabilistic analysis of representative volume element size. Probabilistic Engineering Mechanics **23**, 307–323 (2008)
[20] Ta, Q.A., Clouteau, D., Cottereau, R.: Modeling of random anisotropic elastic media and impact on wave propagation. European Journal of Computational Mechanics **19**, 241–253 (2010)
[21] Torquato, S.: Random Heterogeneous Materials: Microstructure and Macroscopic Properties. Springer, New-York (2002)

[22] Tootkaboni, M., Graham-Brady, L. L.: A multi-scale spectral stochastic method for homogenization of multi-phase periodic composites with random material properties. International Journal of Numerical Methods in Engineering, **83**, 59–90 (2010)
[23] Verlet, L.: Computer "Experiments" on Classical Fluids. I. Thermodynamical Properties of Lennard-Jones Molecules. Physical Review **159**, 98–103 (1967)
[24] Walpole, L. J.: Fourth-rank tensors of the thirty-two crystal classes: Multiplication tables. Proc. R. Soc. Lond. A **391**, 149–179 (1984)
[25] Zohdi, T. I., Wriggers, P.: Introduction To Computational Micromechanics. Springer, New-York (2005)